NJC

Accepted Manuscript

This is an *Accepted Manuscript*, which has been through the Royal Society of Chemistry peer review process and has been accepted for publication.

Accepted Manuscripts are published online shortly after acceptance, before technical editing, formatting and proof reading. Using this free service, authors can make their results available to the community, in citable form, before we publish the edited article. We will replace this *Accepted Manuscript* with the edited and formatted *Advance Article* as soon as it is available.

You can find more information about *Accepted Manuscripts* in the **Information for Authors**.

Please note that technical editing may introduce minor changes to the text and/or graphics, which may alter content. The journal's standard **Terms & Conditions** and the **Ethical guidelines** still apply. In no event shall the Royal Society of Chemistry be held responsible for any errors or omissions in this *Accepted Manuscript* or any consequences arising from the use of any information it contains.

Journal Name

ARTICLE

Solid phase extraction of doxorubicin using molecularly imprinted polymer coated magnetite nanospheres prior to its spectrofluorometric determination

Mazaher Ahmadi, Tayyebeh Madrakian[*], and Abbas Afkhami

This work reports on the synthesis of a doxorubicin-imprinted polymer nanoadsorbent (DOXMNSs). The imprinted polymer was coated on the magnetite nanospheres surface. The synthesized DOXMNSs have been characterized using FT-IR, XRD and TEM measurements. The prepared nanoadsorbent could well disperse in sample medium and, under the optimum condition, can selectively remove the drug from aqueous medium before its magnetic separation. The optimum pH (i.e. pH=7.5) has good match with normal cellular fluid pH and the removal efficiency decreased significantly by pH decreasing. The results give promise of a magnetic drug carrier for cancer therapy purposes. On the other hand, using the proposed method, sensitive doxorubicin determination in the linear concentration range 2.0 - 150.0 ng mL^{-1} with a detection limit of 1.3 ng mL^{-1} could be achievable. The urine samples analyses results showed that a powerful method for the drug determination has been proposed.

Introduction

Doxorubicin (DOX) belongs to a family of anthracycline antibiotics and it is known as an anticancer (antineoplastic) chemotherapy drug, commercialized in the form of chloride salt and sold as Adriamycin.[1-3] The drug displays a broad spectrum of antitumor activity, including activity against acute leukemias, Hodgkin's and Non-Hodgkin's lymphomas, breast cancer, lung cancers, and sarcomas.[3] The mechanisms for the anticancer and toxic effects of DOX include DNA intercalation and strand breakage, inhibition of topoisomerase II, formation of metal complexes with iron or copper, and free radical formation [4, 5]. Clinical use of DOX is limited for its cardiotoxicity that is usually caused by oxidative stress. Like all anthracyclines, DOX primarily works by intercalating DNA, but the mechanism of toxicity is also based on cells damage induced by reactive oxygen species, a mechanism in which free iron plays an important role [1].

From a medical or clinical point of view, monitoring drug levels in body fluids such as urine and plasma has become increasingly demanded in order to assess toxicity, adverse effects, interactions and therapeutic efficiency. So, the development of sensitive and reliable analytical methods for the determination of DOX is a basic requirement for the study of this analyte in different types of samples with complex matrices. For this purpose, different analytical techniques have been used, and the most common among them is high performance liquid chromatography (HPLC) coupled with different detectors such as UV-vis [6], tandem MS [7], chemiluminescence [8], fluorimetric [9], and electroanalytical [10] detectors. Besides these HPLC methods, UV-vis spectrophotometry [11], fluorimetry [12, 13], Raman spectroscopy [14], immunoassay analysis [15], and electroanalytical measurement techniques [16, 17], have also been used for the determination of DOX in different samples. Although these methods have been successfully applied to the analysis of DOX in various matrices, some of these methods lack sensitivity, selectivity and suffer from tedious procedure, are time consuming or high cost.[11, 18-20]

Sample preparation is crucial for obtaining meaningful results from the analysis of real samples, since it is the most tedious and time-consuming step and a possible source of imprecision and inaccuracy of the overall analysis. Nowadays, solid-phase extraction (SPE) is widely used for the extraction and preconcentration of analytes in various environmental, food and biological samples.[21-28] It is the most popular clean-up technique due to factors such as convenience, cost, time saving and simplicity, and it is the most accepted sample pre-treatment method todays [29]. At present, there are several types of sorbents for SPE. However, due to their unsatisfactory

selectivity, these traditional sorbents usually cannot separate analytes efficiently in complex biological or environmental samples [30]. New SPE sorbents have recently appeared as alternatives to conventional solid-phase extraction sorbents with the aim of achieving a more selective preconcentration of the analytes.
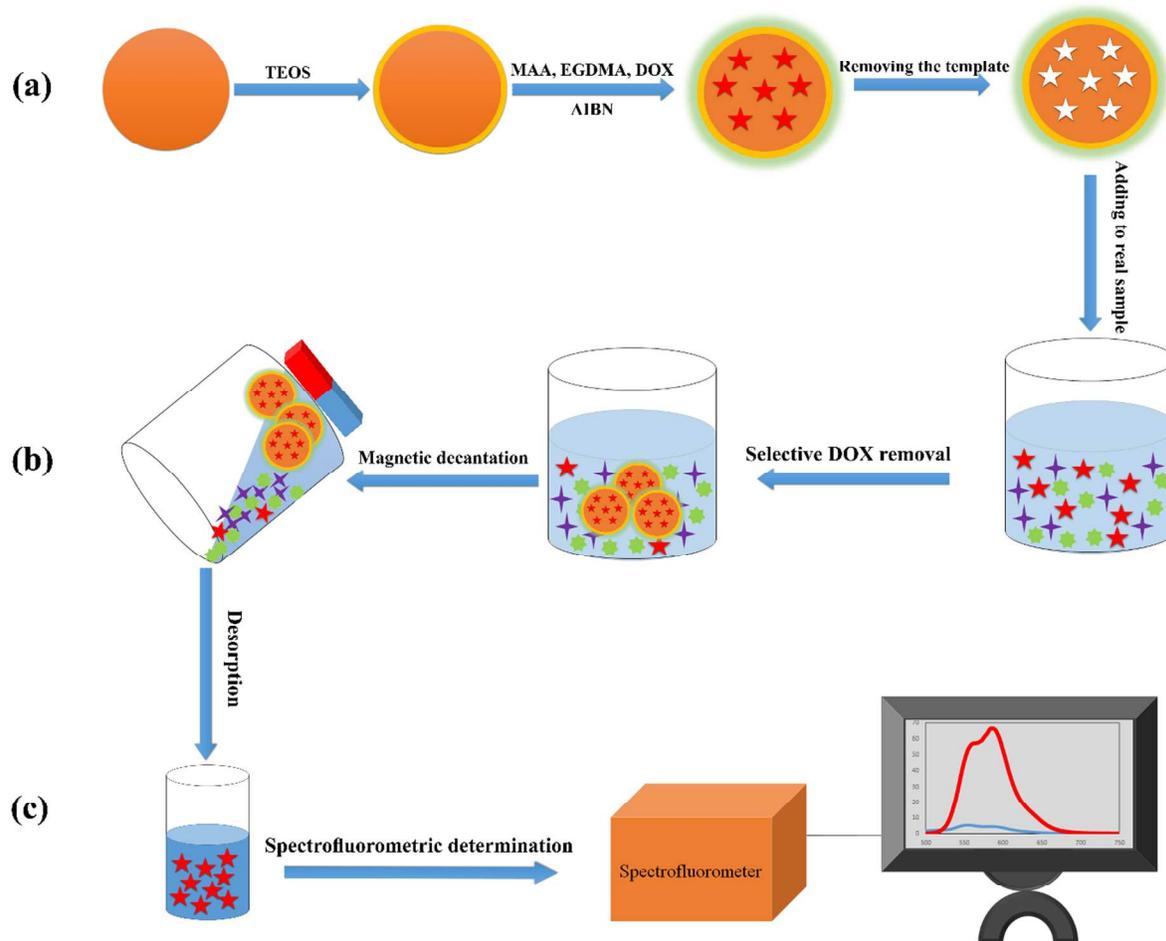
Scheme 1 Overall description of the steps involving in the drug determination: (a) synthesis of the adsorbent, (b) selective removal of the drug and (c) preconcentration and spectrofluorometric determination.

Molecular imprinting has become an established technique for preparing robust molecular recognition elements for a wide variety of target molecules.[31-37] Molecularly imprinting polymers (MIPs) have been investigated as the highly selective sorbents for SPE in order to concentrate and clean up samples prior to analysis. MIPs, involving the formation of cavities in a synthetic polymer for a template analyte, are useful for selective extraction. This analytical method is a rapidly developing technique for preparation polymeric materials that are capable of high molecular recognition.[38, 39] Radical polymerization is usually used for cross-linking of the functional monomers in the presence of template structures and then removing the target (Scheme 1). The use of MIPs for SPE involves conventional SPE where the MIPs is packed into columns or cartridges [40, 41] and batch mode SPE in which the MIPs is incubated with the sample [32]. A major advantage of MIP-based SPE, related to the high selectivity of the sorbent, is achievement of an efficient sample clean-up.

This work reports on the synthesis of a DOX imprinted polymer coated magnetic nanoadsorbent for selective solid phase extraction of DOX from human urine samples. The concentration of DOX in the extract was determined using fluorescence spectroscopy measurement. This procedure is simple, rapid, selective and sensitive. It can be noticed that many works have been published on the determination of DOX, including, conventional spectrofluorimetry.[12, 13] However, the present method is more sensitive as compared with previous ones.[18, 19, 42, 43]

Experimental

Reagents and materials

All the chemicals used were of analytical reagent grade or highest purity available and were purchased from Merck Company (Darmstadt, Germany). Doxorubicin hydrochloride purchased from Sigma-Aldrich Company. Double distilled

water (DDW) was used throughout the work. All glassware were soaked in dilute nitric acid for 12 h and then thoroughly rinsed with DDW. The DOX stock solution was prepared in DDW from its hydrochloride salt and working standard solutions of different DOX concentrations were prepared daily by diluting the stock solution with DDW. Britton-Robinson universal buffer was used for pH adjustments.

Apparatus

The size, morphology and structure of the synthesized nanospheres were characterized by transmission electronic microscopy (TEM, Philips-CMC-300 KV). The crystal structure of the synthesized nanospheres was determined by an X-ray diffractometer (XRD, 38066 Riva, d/G. via M. Misone, 11/D (TN) Italy) at ambient temperature. The magnetic properties of the synthesized nanospheres were measured with a vibrating sample magnetometer (VSM, 4 in. Daghigh Meghnatis Kashan Co., Kashan, Iran). The mid-infrared spectra of the synthesized nanospheres in the region 4000-400 cm^{-1} were recorded by an FT-IR spectrometer (Perkin-Elmer model Spectrum GX) using KBr pellets. A Perkin Elmer (LS50B) luminescence spectrometer was used for DOX spectrofluorometric concentration determination. A Metrohm model 713 pH-meter was used for pH measurements. A 40 kHz universal ultrasonic cleaner water bath (RoHS, Korea) was used.

Synthesis of investigated nanospheres (Scheme 1a)

DOX have been imprinted onto magnetite nanospheres surface, as magnetic carrier, as follows:

SYNTHESIS OF MAGNETITE NANOSPHERES (MNSS)

MNSs were synthesized by solvothermal reduction method with minor modifications [44]. Typically, $FeCl_3.6H_2O$ (1.35 g) was dissolved in ethylene glycol (40.0 mL) to form a clear solution, followed by the addition of sodium acetate (3.6 g) and polyethylene glycol (1.0 g). The mixture was ultrasonicated vigorously for 30.0 min and then refluxed at 180℃ for 8 h, and then allowed to cool down to room temperature. The black products were washed several times with ethanol and DDW water. Then dried at 60℃ for 6 h.

SYNTHESIS OF SILICA COATED MAGNETITE NANOSPHERES (SCMNSS)

SCMNSs were prepared according to the previously reported method with minor modifications [45]. Typically, 0.5 g of MNSs was dispersed in 60.0 mL ethanol and 10 mL DDW by sonication for 15 min, followed by the addition of 1.0 mL ammonium hydroxide (25%) and 3.0 mL tetraethoxysilane sequentially. The mixture was reacted for 12 h at room temperature under the continuous stirring. The resultant product was collected by an external magnetic field, and rinsed consecutively six times with ethanol and DDW. Finally, the obtained SCMNSs were dried under vacuum at 60℃ for 3 h.

SYNTHESIS OF DOX IMPRINTED POLYMER COATED MAGNETITE NANOSPHERES (DOXMNSS)

Typically 3 mmol of MAA (Methacrylamide, as the functional monomer), 20 mmol of EGDMA (Ethylene glycol

dimethacrylate, as the cross-linker), and 400.0 mg of SCMNPs agent were dispersed into a 45.0 mL acetonitrile solution of DOX (1 mmol, as the template). After sealing, shaking, and purging the mixture with nitrogen, a 5.0 mL acetonitrile solution with 50.0 mg of AIBN (2-2'-azoisobutyronitrile, as the initiator) was added into the suspension with a sample injector. The resultant mixture was ultrasonicated at 60 ℃ for 2 h under the nitrogen protection and then stirred overnight. The product was washed with the mixture of methanol: 1.0 mol L^{-1} acetic acid (1:1 v/v) until no template molecule (DOX) was detected spectrofluorometrically in the washing solution. Then, the product (DOXMNSs) was separated by a magnet and washed overnight with the mixture of methanol: 1.0 mol L^{-1} acetic acid (1:1 v/v). Then, the resulting nanospheres were dried under the vacuum for 12 h. As a reference, non-imprinted polymer coated SCMNPs (NIPMNPs), which did not contain the template, was also prepared in parallel with the DOXMNSs by using the same synthetic protocol in the absence of the template.

DOX removal experiments (Scheme 1b)

To a 25.0 mL sample solution containing DOX and 10.0 mL Britton-Robinson buffer solution of pH 7.5, a 0.02 g of DOXMNSs was added. The solution was shaken at room temperature for 25.0 min. Subsequently, the DOX loaded DOXMNSs were separated from the mixture with a permanent hand-held magnet within 60 s. The residual amount of the drug in the solution was determined spectrofluorometrically at λ_{em}= 558 nm (λ_{ex}= 462 nm) (Emission and excitation spectra of DOX are shown in Fig. 1). The adsorption percentage, i.e., the drug removal efficiency (%Re), was determined using the following equation:

$$\%Re = \left[\frac{(C_0 - C_t)}{C_0} \right] \times 100 \tag{1}$$

where C_o and C_t represent the initial and final (after adsorption) concentrations of the drug in mg L^{-1}, respectively. Also all the experiments were performed at room temperature.
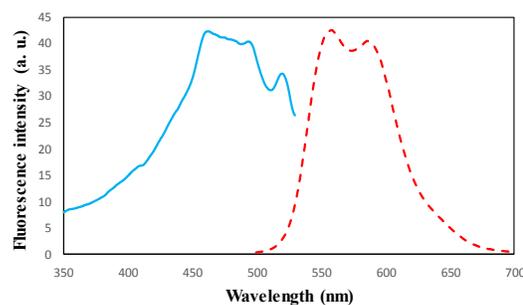
Fig. 1 Fluorescence excitation (—) at λ_{em}=558 nm and emission spectra (- - -) at λ_{ex}=462 for DOX in water at pH 7.5 at room temperature.

DOX preconcentration and spectrofluorometric determination (Scheme 1c)

Preconcentration studies for the determination of trace amounts of DOX were performed by adding 250.0 mL of the

solution containing 2.0-150.0 ng mL^{-1} of DOX and 150 mL of Britton-Robinson buffer of pH 7.5 to 0.02 g of DOXMNSs and the solution was stirred for 25 min. The concentration of DOX decreased with time due to the adsorption by DOXMNSs. The DOX loaded nanospheres were separated with magnetic decantation and desorption was performed with a 2.0 mL of the mixture of methanol: 1.0 M acetic acid (1:1 v/v). The concentration of DOX in the resulting solution was measured spectrofluorometrically at λ_{em}= 555 nm (λ_{ex}= 462 nm).

Urine samples pretreatment

Drug-free urine samples were collected from healthy donors. All urine samples were stored at -20 ^{o}C. Then, 50.0 mL of each sample was diluted with 150 mL of Britton-Robinson buffer of pH 7.5 solution and 50.0 mL of DDW and directly subjected to the SPE procedure (section 2.5). Urine samples were spiked with DOX at ng mL^{-1} concentrations levels.

Results and discussion

In order to synthesis DOXMNSs, firstly MNSs were synthesized by solvothermal reduction method. Then the synthesized nanospheres were coated with a layer of SiO$_2$ using TEOS silanization agent. Finally, the synthesized SCMNSs surface DOX imprinted using MAA as the functional monomer, EGDMA as the cross-linker, DOX as the template and AIBN as the polymerization reaction initiator

Characterization of the investigated nanospheres

The magnetization curves of the bare MNSs, SCMNSs and DOXMNSs recorded with VSM are illustrated in Fig. 2. As shown in Fig. 2, the magnetization of the samples would approach the saturation values when the applied magnetic field increases to 10,000 Oe. The saturation magnetization of the MNSs was 41.47 emu/g. For SCMNSs and DOXMNSs, the saturation magnetization were 30.13 and 27.19 emu/g, respectively. These results showed that magnetic properties are hardly affected by the surface modification. A magnetization reduction of about 27.34% was observed between the bare and SiO$_2$-coated Fe$_3$O$_4$ nanospheres (SCMNSs), and about 9.76% between SCMNSs and DOXMNSs. This may be related to the nanospheres size effect, the increased surface disorder, and the diamagnetic contribution of SiO$_2$ and imprinted polymer layers.
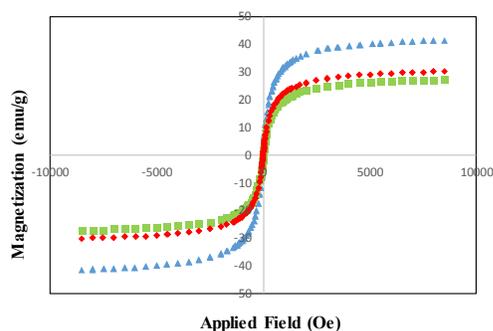
Fig. 2 Magnetization curves obtained by vibrating sample magnetometer at room temperature: (▲) bare MNSs; (♦) SCMNSs; and (■) DOXMNSs nanospheres.

The FTIR spectra for the products in each step of the DOXMNSs synthesis were recorded to verify the formation of the expected products. The related spectra are shown in Fig. 3. The characteristic absorption band of Fe-O in Fe$_3$O$_4$ (around 580 cm^{-1}) is observed in Fig. 3a. A strong peak at about 1090 cm^{-1} in Fig. 3b is attributed to Si-O in SiO$_2$. Two new absorption peaks at 1723 cm^{-1} and 1252 cm^{-1} in Fig. 3c are assigned to C=O and C-N bands in the polymer-coated final product (DOXMNSs), respectively.. Moreover, new absorption peaks at 2819 and 2857 cm^{-1} are related to the stretching modes of aliphatic C-H bonds in final product [21]. The peaks at about 3300 cm^{-1} are attributed to water and the nanospheres surface hydroxyl groups. Based on the above results, it can be concluded that the fabrication procedure has been successfully performed.
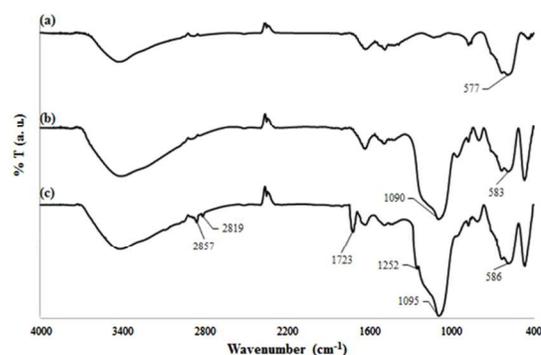
Fig. 3 FT-IR spectra for (a) MNSs, (b) SCMNSs and (c) DOXMNSs nanospheres.

The XRD pattern of DOXMNSs (Fig. 4) shows diffraction peaks that are indexed to (2 2 0), (3 1 1), (4 0 0), (4 2 2), (5 1 1), (4 4 0) and (5 5 3) reflection characteristics of the cubic spinel phase of Fe$_3$O$_4$ (JCPDS powder diffraction data file no. 79-0418), revealing that the resultant nanospheres are mostly Fe$_3$O$_4$. The average crystallite size of the DOXMNSs nanospheres was estimated to be 10 nm from the XRD data according to Scherrer equation [24].
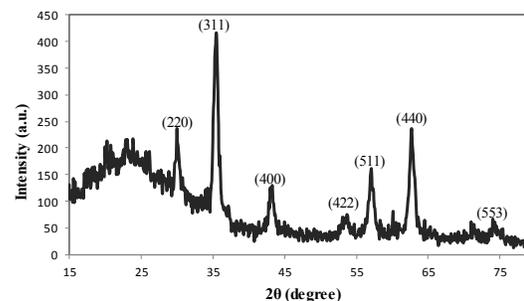
Fig. 4 XRD pattern for DOXMNSs nanospheres.

The TEM image of the MNSs in Fig. 5a indicates that spherical monodisperse nanoparticles with an average diameter

of about 90 nm were synthesized. Figure 5b indicates that MNSs successfully coated with a core-shell layer of SiO_2. Figure 5c depicts DOXMNSs nanospheres. The Figures show that after MIP layer coating process, core-shell layer thickness and morphological properties have been to some extent changed.

Point of zero charge (pH_{PZC}) of DOXMNSs nanospheres

The pH_{PZC} of the DOXMNSs was determined in degassed 0.01 mol L^{-1} $NaNO_3$ solution at room temperature. Aliquots of 30.0 mL 0.01 mol L^{-1} $NaNO_3$ were mixed with 0.03 g of the nanospheres in several beakers. The initial pH of the solutions were adjusted at 3.0, 4.0, 5.0, 6.0, 7.0, 8.0, 9.0 and 10.0 using 0.01 mol L^{-1} of HNO_3 and/or NaOH solutions as appropriate. The initial pHs of the solutions were recorded, and the beakers were covered with parafilm and shaken for 24 h. The final pH values were recorded and the differences between the initial and final pH (ΔpH) of the solutions were plotted against their initial pH values. The pH_{PZC} corresponds to the pH where $\Delta pH=0$ [31]. The pH_{PZC} for DOXMNSs was determined using the above procedure and was obtained as 6.3. The results are shown at Fig. 6.
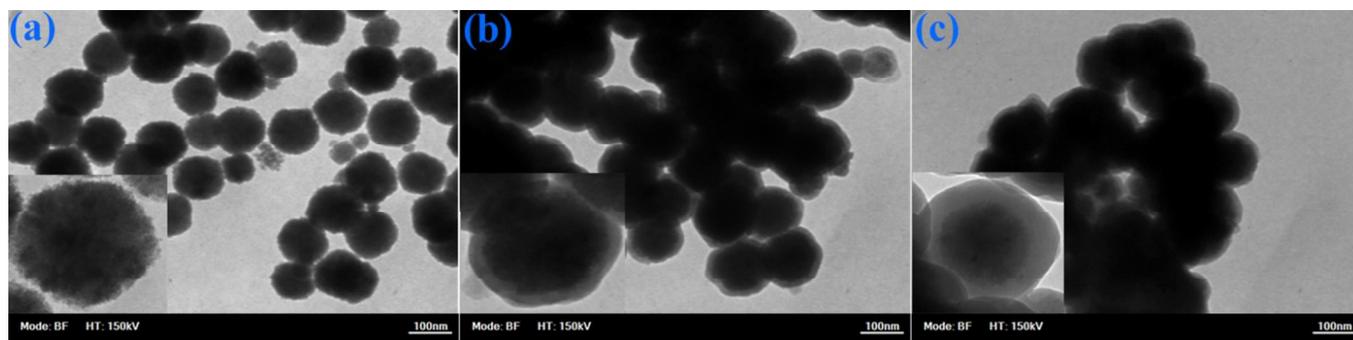
Fig. 5 TEM images for (a) MNSs, (b) SCMNSs and (c) DOXMNSs nanospheres.
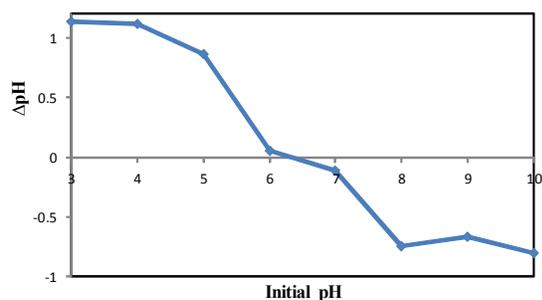
Fig. 6 Point of zero charge (pH_{pzc}) of DOXMNSs nanospheres.

Effect of various factors affecting the DOX removal efficiency step

Various factor that can potentially affect the drug removal efficiency (i.e. pH, contact time and nanospheres dosage) were optimized using "one-at-a-time" method. Here are the detailed results:

EFFECT OF PH

One of the important factors affecting the removal of the drug from aqueous solutions is the pH of the solution. The dependence of the drug sorption on pH is related to both the drug chemistry in the solution and the ionization state of the functional groups of the sorbent which affects the availability of binding sites. Drug chemistry usually depends on its pK_a (or pK_b) that one can predict ionization state of acidic or basic functional groups of the molecule at each pH. In the case of the adsorbent, responsible parameter is point of zero charge

(pH_{PZC}). The point of zero charge is a characteristic of the metal oxides (hydroxides) and of fundamental importance in surface science. It is a concept relating to the phenomenon of adsorption and describes the condition when the electrical charge density on a surface is zero. The surface charge of DOXMNSs with primary amine groups (belongs to amid group of the functional monomer) and hydroxyl groups (belongs to SiO_2 core-shell layer that been partially covered by MIP layer) is largely dependent on the pH of the solution. The pH_{PZC} caused by the amphoteric behaviour of hydroxyl and amino surface groups, and the interaction between surface sites and the electrolyte species. When brought into contact with aqueous solutions, hydroxyl groups of surface sites can undergo protonation or deprotonation, depending on the solution pH, to form charged surface species.
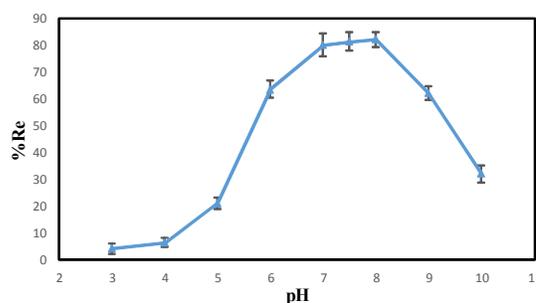
Fig. 7 Removal efficiency of DOX at different pHs (Conditions: 0.01 g of DOXMNSs, 25 mL of 20.0 mg L^{-1} of DOX, agitation time of 45 min).

The effect of pH on the DOX removal efficiency was investigated in the range 3.0–10.0 using an initial DOX

concentration of 20.0 mg L^{-1} and a stirring time of 45 min, where the pH was adjusted with Britton-Robinson buffer. Figure7 indicates that the adsorbent provided highest affinity to DOX at pH 7.5. This is reasonable, because the only species significantly present in the region between Hammett acidity -4.0 and pH 8.0 is the singly charged species with the positive charge at the amino sugar group (at Hammett acidity<-4.0 only monocation of D can significantly present). However, at a pH greater than 8.0, this monocation (C) can lose a proton either from a phenolic group to form a zwitterion (Z) or from the amino sugar group to form the neutral species (N). Either may then lose a proton to form the singly charged anion (A)

(Scheme 2 [46]). On the other hand, the adsorbent surface charge at pH<6.3 (pH_{PZC}=6.3) is positive and electrostatic repulsion is responsible for low DOX removal efficiency. But at pH range 6.3-8.0, the adsorbent surface charge is negative and the electrostatic attraction forces are responsible for high removal efficiency of the positively charged DOX molecules. At pH>8.0, the electrostatic repulsion between the negatively charged adsorbent surface and DOX anions should be probably responsible for the decrease in DOX removal efficiency. It should be noted that at these pHs DOX is partially in its neutral form and this is another reason for removal efficiency decreasing due to electrostatic attraction forces lost.
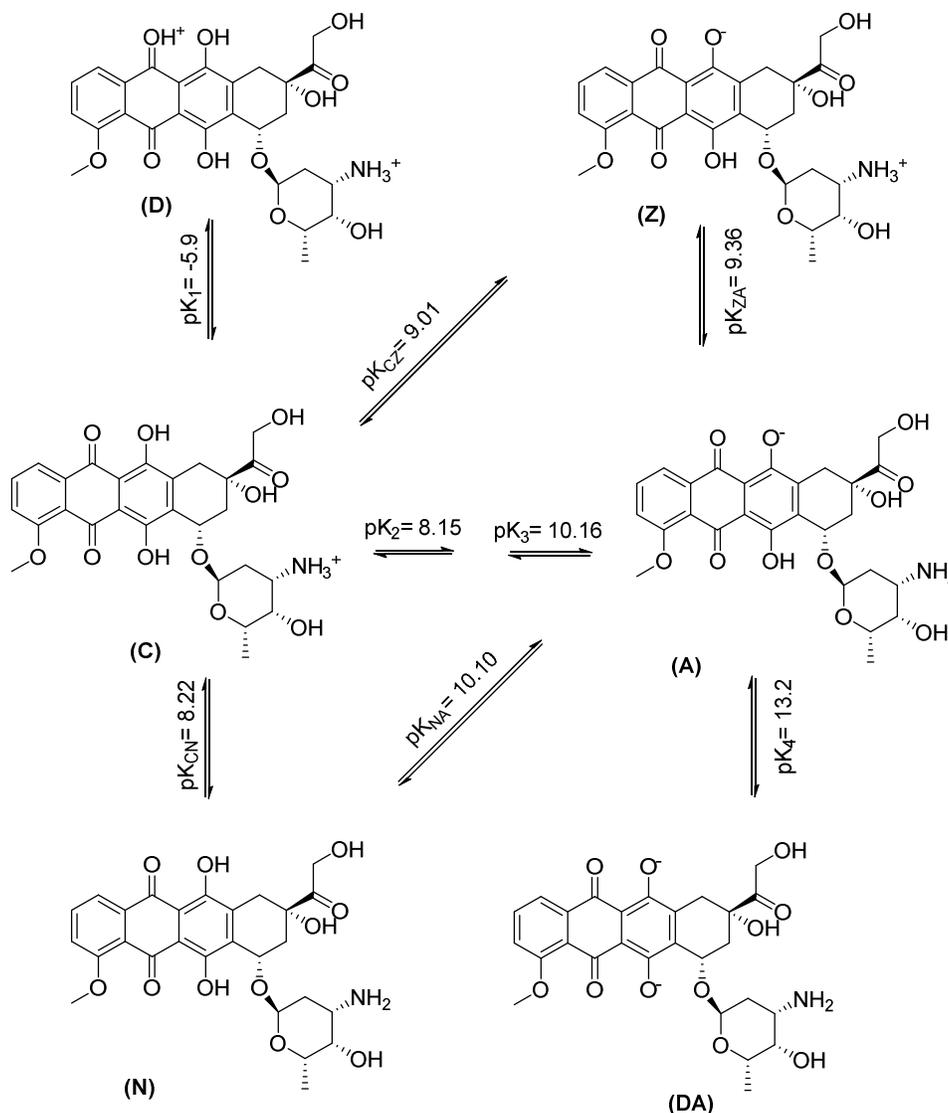
Scheme 2 Overall dissociation pathway and negative logarithms of dissociation constants of doxorubicin

The optimum pH has good match with normal cellular physiological pH (i.e. pH=7.5) and removal efficiency significantly decreased by pH decreasing. The pH-sensitive desorption of the synthesized nanospheres enabling it to release active drug in target tissues in which the pH is less than physiologic values [47], such as in the acidic environment of

tumor cells. At the other hand, magnetic properties of the nanospheres give us the ability of targeted drug delivery to desired tissues with pre-applied magnetic field. These results can promise a magnetic drug carrier for cancer therapy purposes after performing the in vivo and in vitro biocompatibility tests.

EFFECT OF NANOSPHERES DOSAGE

The dependence of the adsorption of DOX on the amount of modified nanospheres was studied at room temperature and at pH 7.5 by varying the adsorbent amount from 0.01 to 0.05 g in contact with 25.0 mL solution of 20.0 mg L^{-1} of DOX with agitation time of 45 min. The results showed that the removal efficiency of DOX increased by increasing the amount of DOXMNSs due to the availability of higher adsorption sites. The adsorption reached a maximum with 0.02 g of adsorbent and maximum percentage removal was about 98%.

EFFECT OF CONTACT TIME

The effect of contact time on the adsorption of DOX was studied to determine the time needed to remove DOX by DOXMNSs from a 20.0 mg L^{-1} solution of the drug at pH 7.5. A 0.02 g of the adsorbent was added into 25.0 mL (containing 10.0 mL of buffer solution of pH 7.5) of the drug solution. Fluorescence intensity of DOX was monitored versus time to determine variation of the drug concentration. It was observed that after a contact time of about 25.0 min, almost all the drug was adsorbed (%Re>98) and this time was much enough to reach semi-equilibrium condition.

Effect of various factors affecting the DOX preconcentration efficiency

The aim of this step is providing the highest preconcentration factor and concentration of the adsorbed drug into minimum possible volume of desorbing solvent. In this regard, various factor that can potentially affect the drug desorbing efficiency (i.e. type and volume of desorbing solvent, desorbing time and initial sample volume) have been optimized using "one-at-a-time" method. The detailed results are given in bellow:

DESORBING SOLVENT (INCLUDE TYPE AND VOLUME OF ELUENT AND DESORBING TIME)

For desorption studies, DOX loaded DOXMNSs were first washed by DDW to remove the unadsorbed DOX that loosely attached to the vial and adsorbent. In order to estimate the recovery of DOX from DOXMNSs, desorption experiments with different reagents (methanol, 1.0 mol L^{-1} acetic acid, mixture of methanol: 1.0 mol L^{-1} acetic acid (1:1 v/v)) were performed. After adsorption of DOX, the adsorbent was magnetically separated and washed with DDW. Then 2.0 mL of the eluent was added to the DOX loaded DOXMNSs. Samples were collected after 5.0, 10.0, 20.0, 30.0 and 45.0 min contact times to evaluate DOX recovery. The results showed that the mixture of methanol with 1.0 mol L^{-1} acetic acid (1:1 v/v) is the most effective as a back-extracting solvent and can be used for the quantitative recovery of the drug. Desorption rate was found to be rapid as almost 98% desorption completed at almost 10.0 min.

INITIAL SAMPLE VOLUME

The effect of initial sample volume on the drug adsorption was studied in the range 25.0–400.0 mL; 25.0 mL samples containing 2.0 mg L^{-1} of DOX were diluted to 25.0, 50.0, 75.0, 100.0, 150.0, 200.0, 250.0, 300.0 and 400.0 mL with DDW. Then adsorption and desorption processes were performed under the optimum conditions (pH 7.5; contact time, 25.0 min; DOXMNSs dosage, 0.02 g) as described in the experimental section. The results showed that the drug content in the volumes up to 250.0 mL was completely and quantitatively adsorbed by the nanospheres, but there was a decrease in the amount adsorbed at higher volumes. Therefore, for the determination of trace quantities of the drug, a sample volume of 250.0 mL was selected in order to having highest preconcentration factor.

Table 1 Adsorption isotherm parameters of Langmuir and Freundlich models for the adsorption of the drug on DOXMNSs and NIPMNPs adsorbents.

Isotherm models	Langmuir					Freundlich			
	K_L (L mg^{-1})	q_{max} (mg g^{-1})	R^2	RMS		K_f	$1/n$	R^2	RMS
DOXMNSs	0.72	59.17	0.9695	0.79		2.85	0.23	0.8236	2.91
NIPMNPs	0.82	15.27	0.8962	1.14		8.86	0.14	0.6462	2.11

Adsorption isotherms

The capacity of the adsorbent is an important factor that determines how much sorbent is required to quantitatively remove a specific amount of the drug from solution. For measuring the adsorption capacity of DOXMNSs and NIPMNPs, the absorbents was added into DOX solutions at various concentrations (under optimum condition), and the suspensions were stirred at room temperature, followed by magnetic removal of the absorbent. An adsorption isotherm describes the fraction of the sorbate molecules that are partitioned between the liquid and the solid phase at equilibrium. Adsorption of the DOX by DOXMNSs adsorbent was modelled using Freundlich [48] and Langmuir [49] adsorption

isotherm models. The remained drug in the supernatants was measured spectrofluorometrically at λ_{em}= 558 nm (λ_{ex}= 462 nm), and the results were used to plot the isothermal adsorption curves as shown in Fig. 8. The equilibrium adsorption data were fitted to Langmuir and Freundlich isotherm models by nonlinear regression. The resulting parameters are summarized in Table 1.

The higher correlation coefficient obtained for the Langmuir model and lower RMS values indicates that the experimental data are better fitted into this model, and adsorption of DOX on DOXMNSs adsorbents is more compatible with Langmuir assumptions, i.e., adsorption takes place at specific homogeneous sites within the adsorbent. The Langmuir model is based on the physical hypothesis that the

maximum adsorption capacity consists of a monolayer adsorption, that there are no interactions between adsorbed molecules, and that the adsorption energy is distributed homogeneously over the entire coverage surface. This sorption model serves to estimate the maximum uptake values where they cannot be reached in the experiments.
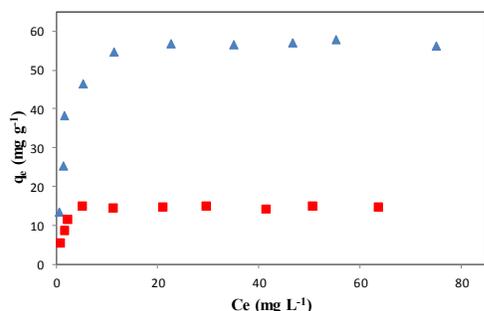
Fig. 8 Isothermal adsorption curves of DOX on (▲) DOXMNSs and (■) NIPMNPs adsorbents.

According to the results (Table 1), the maximum amount of DOX that can be adsorbed by DOXMNSs and NIPMNPs was found to be 59.17 and 15.27 mg g^{-1} at pH 7.5, respectively. The relatively high adsorption capacity of DOXMNSs in comparison with NIPMNPs, shows that the adsorption of DOX molecules takes place at a large number of specific homogeneous sites within the adsorbent (specific cavities of the MIP), besides non-specific interactions which are approximately identical for both DOXMNSs and NIPMNPs adsorbents.

Reusability and stability of the adsorbent

The reusability and stability of DOXMNSs for the extraction of DOX was assessed by performing eleven consecutive separations/desorption cycles under the optimized conditions (Conditions: 0.02 g of DOXMNSs, 25.0 mL of 2.0 mg L^{-1} of DOX, agitation time of 25 min). Desorption of DOX from the adsorbent was performed with a mixture of methanol: 1.0 mol L^{-1} acetic acid (1:1 v/v) as described in the experimental section. There was no significant change in the performance of the adsorbent during these eleven cycles,

indicating that the fabricated DOXMNSs is a reusable and stable solid phase sorbent for the extraction of DOX.

Analytical application

Calibration graph was constructed from spectrofluorometric measurements of the desorbed DOX after performing its adsorption/separation under the optimum conditions described above. The calibration graph was linear in the range 2.0 - 150.0 ng mL^{-1} for a sample volume of 250.0 mL. The calibration equation is $I_F = 0.6211C + 0.2511$ with a determination coefficient of 0.9975 (n = 8), where I_F is the fluorescence intensity of the eluate at $\lambda_{em}= 555$ nm ($\lambda_{ex}= 462$ nm) and C is the concentration of the drug in ng mL^{-1}. The limit of detection, defined as LOD $=3S_b$ /m, where LOD, S_b and m are the limit of detection, standard deviation of the blank and the slope of the calibration graph, respectively, was found to be 1.3 ng mL^{-1} of DOX. As the drug in 250.0 mL of the sample solution was concentrated into 2.0 mL, a maximum preconcentration factor of 125.0 was achieved in this method. The relative standard deviations (RSD) for 100.0 and 5.0 ng mL^{-1} of the drug were 0.82% and 1.41% (n = 3), respectively.

Table 2 Assay of DOX in human urine samples by means of the proposed method (n=3).

Sample	Spiked value (ng mL^{-1})	Found (ng mL^{-1})	Recovery percent
1	10.00	9.61 ± 0.11	96.10
2	30.00	31.10 ± 1.02	103.67
3	75.00	74.34 ± 0.86	99.12
4	130.00	132.41 ± 0.77	101.85

The analytical applicability of the proposed method was evaluated by determining the DOX content of different amounts of DOX spiked healthy human urine samples using DOXMNSs adsorbent. The results are given in Table 2.

The results show good recoveries of the proposed method for the DOX added to urine samples and the method is a good candidate for DOX determination in urine samples. Since only 5.9% of DOX were excreted by the kidney during the initial 48 hours[50], concentration of DOX in urine must be at low levels in comparison to its plasma concentration level. So, low LOD value of the proposed method can be considered when dealing with DOX determination in urine samples.

Table 3 Comparison of the proposed method with the reported methods for DOX determination.

Method	LOD (ng mL^{-1})	Linear range (ng mL^{-1})	Sample	Ref.
EEM-PARAFAC[a]	32[g]	-	Human plasma	[42]
TSFS[b]	10[g]	-	Human plasma	[43]
pH-gradient flow-injection[c]	770[g]	1500-12000[g]	Human plasma	[18]
AdSWV[d]	1.50	4.99-59.64	Human urine	[1]
DLR[e]	217.4[h]	-	Human urine	[19]
SPE/HPLC/MS[f]	0.04	0.1-2.0	Human urine	[20]
MIP/SPE/FL	1.3	2.0 - 150.0	Human urine	This work

[a] Excitation–emission matrix fluorescence measurements and multi-way chemometric methods based on parallel factor analysis.
[b] Total synchronous fluorescence spectroscopic data modelled with first- and second-order algorithms.
[c] Second-order spectrophotometric data generated by a pH-gradient flow injection technique.
[d] Adsorptive square-wave voltammetry.
[e] Dual lifetime referenced fluorometry.
[f] Solid phase extraction/ high-performance liquid chromatography/tandem mass spectrometry.
[g] Concentration have been originally reported as μg mL^{-1} unit.
[h] Concentration have been originally reported as μmol L^{-1} unit.

Journal Name

ARTICLE

Table 3 shows a comparison between the results obtained by the present method with those obtained by some other methods reported for the determination of DOX.

In this comparison, the determination of DOX by HPLC in combination with mass spectrometry with SPE sample preparation method (SPE/HPLC/MS) yielded the lowest LOD. Such measurements, however, depend on expensive instrumentation and are costly to operate. By contrast, it is much simpler and less expensive to measure the intrinsic fluorescence of the drug after preconcentration using the proposed MIP adsorbent. Other advantages of the proposed method are low LOD, wide linear range, simplicity and high removal capacity of the adsorbent. The major advantage of the magnetic adsorbents is easy separation of the adsorbent after completion of the drug removal process. On the other hand, consumption of very small volumes of low toxic organic solvents in comparison to HPLC methods, is another advantage of the proposed method.

Conclusion

A selective DOX-imprinted polymer coated magnetite nanospheres were synthesized. The preparation of this material was relatively simple and rapid. The synthesized magnetic nanospheres could well dispersed in sample medium and subsequently easily removed from medium after surface adsorption of DOX drug. DOX removal and preconcentration results showed that under optimum condition, sensitive DOX fluorimetric determination in the linear concentration range of 2.0 - 150.0 ng mL^{-1} with LOD of 1.3 ng mL^{-1} was achievable. This study indicated that the sorption of DOX onto the imprinted polymer was much better than that on non-imprinted polymer. The imprinted polymer also presents the advantages of high adsorption capacity and high chemical stability. The proposed method was successfully applied to the analysis of DOX in the human urine samples and the results showed that the method is a powerful ones for DOX determination in comparison to previously reported method. Finally, the pH-sensitive desorption behavior of the synthesized nanospheres can gives promise of a magnetic drug carrier for cancer therapy purposes after performing the in vivo and in vitro biocompatibility tests.

Acknowledgements

Notes

Faculty of Chemistry, Bu-Ali Sina University, Hamedan, Iran
Corresponding author, Tel. / Fax: +98-811-8380709
E. mail address: madrakian@basu.ac.ir, madrakian@gmail.com

References

1. O. Vajdle, J. Zbiljić, B. Tasić, D. Jović, V. Guzsvány and A. Djordjevic, *Electrochim. Acta*, 2014, **132**, 49.
2. R. H. Blum and S. K. Carter, *Ann. Intern. Med.*, 1974, **80**, 249.
3. D. L. Chin, B. L. Lum and B. I. Sikic, *J. Chromatogr. B*, 2002, **779**, 259.
4. G. P. Sartiano, W. E. Lynch and W. D. Bullington, *T J. Antibiot.*, 1979, **32**, 1038.
5. J. W. Lown, *Pharmacol. Ther.*, 1993, **60**, 185.
6. D. L. Chin, B. L. Lum and B. I. Sikic, *J. Chromatogr. B*, 2002, **779**, 259.
7. R. D. Arnold, J. E. Slack and R. M. Straubinger, *J. Chromatogr. B*, 2004, **808**, 141.
8. S. Ahmed, N. Kishikawa, K. Ohyama, M. Wada, K. Nakashima and N. Kuroda, *Talanta*, 2009, **78**, 94.
9. A. Kümmerle, T. Krueger, M. Dusmet, C. Vallet, Y. Pan, H. B. Ris and L. A. Decosterd, *J. Pharm. Biomed. Anal.*, 2003, **33**, 475.
10. R. Ricciarello, S. Pichini, R. Pacifici, I. Altieri, M. Pellegrini, A. Fattorossi and P. Zuccaro, *J. Chromatogr. B*, 1998, **707**, 219.
11. L. B. Liao, H. Y. Zhou and X. M. Xiao, *J. Mol. Struct.*, 2005, **749**, 108.
12. Y. Liu and B. Danielsson, *Anal. Chim. Acta*, 2007, **587**, 47.
13. K. K. Karukstis, E. H. Z. Thompson, J. A. Whiles and R. J. Rosenfeld, *Biophys. Chem.*, 1998, **73**, 249.
14. Q. Yan, W. Priebe, J. B. Chaires and R. S. Czernuszewicz, *Biospectroscopy*, 1997, **3**, 307.
15. K. Hirano, T. Nagae, T. Adachi, Y. Ito and M. Sugiura, *J. Pharmacobiodyn.*, 1983, **6**, 588.
16. E. A. Hillard, F. C. de Abreu, D. C. M. Ferreira, G. Jaouen, M. O. F. Goulart and C. Amatore, *Chem. Commun.*, 2008, DOI: 10.1039/B718116G, 2612-2628.
17. Š. Komorsky-Lovrić, *Bioelectrochem.*, 2006, **69**, 82.
18. M. R. Alcaráz, A. V. Schenone, M. J. Culzoni and H. C. Goicoechea, *Microchem. J.*, 2014, **112**, 25.
19. F. Martínez Ferreras, O. S. Wolfbeis and H. H. Gorris, *Anal. Chim. Acta*, 2012, **729**, 62.
20. C. Sottani, G. Tranfo, M. Bettinelli, P. Faranda, M. Spagnoli and C. Minoia, *Rapid Commun. Mass Spectrom.*, 2004, **18**, 2426.
21. T. Madrakian, A. Afkhami, M. A. Zolfigol, M. Ahmadi and N. Koukabi, *Nano-Micro Lett.*, 2012, **4**, 57.
22. T. Madrakian, A. Afkhami, M. Rahimi, M. Ahmadi and M. Soleimani, *Talanta*, 2013, **115**, 468.

23. T. Madrakian, A. Afkhami, H. Mahmood-Kashani and M. Ahmadi, *J. Iran. Chem. Soc.*, 2013, **10**, 481.

24. T. Madrakian, A. Afkhami and M. Ahmadi, *Chemosphere*, 2013, **90**, 542.

25. A. Afkhami, R. Moosavi and T. Madrakian, *Talanta*, 2010, **82**, 785.

26. A. Afkhami, H. Bagheri and T. Madrakian, *Desalination*, 2011, **281**, 151.

27. M. Roldán-Pijuán, R. Lucena, S. Cárdenas and M. Valcárcel, *Microchem. J.*, 2014, **115**, 87.

28. M. Cai, X. Chen, X. Wei, S. Pan, Y. Zhao and M. Jin, *Food Chem.*, 2014, **158**, 459.

29. M. Javanbakht, A. M. Attaran, M. H. Namjumanesh, M. Esfandyari-Manesh and B. Akbari-adergani, *J. Chromatogr. B*, 2010, **878**, 1700.

30. C. He, Y. Long, J. Pan, K. Li and F. Liu, *J. Biochem. Bioph. Methods*, 2007, **70**, 133.

31. T. Madrakian, A. Afkhami, H. Mahmood-Kashani and M. Ahmadi, *Talanta*, 2013, **105**, 255.

32. T. Madrakian, M. Ahmadi, A. Afkhami and M. Soleimani, *Analyst*, 2013, **138**, 4542.

33. A. Afkhami, H. Ghaedi, T. Madrakian, M. Ahmadi and H. Mahmood-Kashani, *Biosens. Bioelectron.*, 2013, **44**, 34.

34. X. Sun, J. Wang, Y. Li, J. Jin, J. Yang, F. Li, S. M. Shah and J. Chen, *J. Chromatogr. A*, 2014, **1360**, 9.

35. W. Rao, R. Cai, Y. Yin, F. Long and Z. Zhang, *Talanta*, 2014, **128**, 170.

36. Y. Shiraishi, T. Suzuki and T. Hirai, *New J. Chem.*, 2010, **34**, 714.

37. X. Su, X. Li, J. Li, M. Liu, F. Lei, X. Tan, P. Li and W. Luo, *Food Chem.*, DOI: http://dx.doi.org/10.1016/j.foodchem.2014.09.024.

38. S. Rimmer, *Chromatographia*, 1998, **47**, 470.

39. S. G. Dmitrienko, V. V. Irkha, A. Y. Kuznetsova and Y. A. Zolotov, *J. Anal. Chem.*, 2004, **59**, 808.

40. J. Olsen, P. Martin and I. D. Wilson, *Anal. Commun.*, 1998, **35**, 13H.

41. A. Zander, P. Findlay, T. Renner, B. Sellergren and A. Swletlow, *Anal. Chem.*, 1998, **70**, 3304.

42. M. G. Trevisan and R. J. Poppi, *Anal. Chim. Acta*, 2003, **493**, 69.

43. A. Schenone, M. Culzoni, A. Campiglia and H. Goicoechea, *Anal. Bioanal. Chem.*, 2013, **405**, 8515.

44. H. Deng, X. Li, Q. Peng, X. Wang, J. Chen and Y. Li, *Angew. Chem. Int. Ed.*, 2005, **44**, 2782.

45. C. L. Fang, K. Qian, J. Zhu, S. Wang, X. Lv and S. H. Yu, *Nanotechnology*, 2008, **19**, 125601.

46. R. J. Sturgeon and S. G. Schulman, *J. Pharm. Sci.*, 1977, **66**, 958.

47. M. B. Yatvin, W. Kreutz, B. A. Horwitz and M. Shinitzky, *Science (New York, N.Y.)*, 1980, **210**, 1253.

48. H. Freundlich and W. Heller, *J. Amer. Chem. Soc.*, 1939, **61**, 2228.

49. I. Langmuir, *J. Amer. Chem. Soc.*, 1916, **38**, 2221.

50. K. Mross, P. Maessen, W. J. van der Vijgh, H. Gall, E. Boven and H. M. Pinedo, *J. Clin. Oncol.*, 1988, **6**, 517.

Table of Contents (TOC)
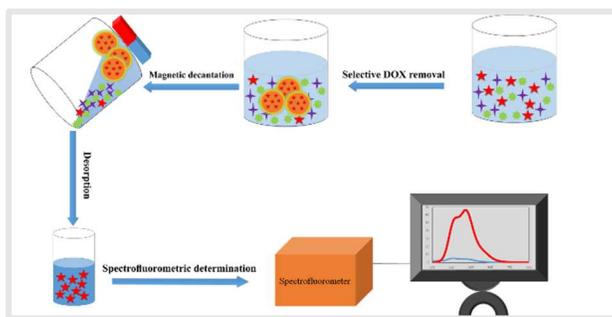
A selective doxorubicin-imprinted polymer coated magnetite nanospheres were synthesized.